NASA CR-145138
BBN Report No. 3379

Measurements of the Reflection Factor of Flat Ground Surfaces

by
C. S. Ventres
M. M. Myles
I. L. Vér

Prepared under Contract No. NAS1-13814
by
Bolt Beranek and Newman Inc.
Cambridge, Mass. 02138

for

NASA

National Aeronautics and
Space Administration
Langley Research Center
Hampton, Virginia 23665

1. Report No.	2. Government Accession No.	3. Recipient's Catalog No.
NASA CR-145138		

4. Title and Subtitle	5. Report Date
MEASUREMENTS OF THE REFLECTION FACTOR OF FLAT GROUND SURFACES	April 1977
	6. Performing Organization Code: ---
7. Author(s): C.S. Ventres, M.M. Myles, I.L. Vér	8. Performing Organization Report No.: 3379
9. Performing Organization Name and Address: Bolt Beranek and Newman Inc. 50 Moulton Street Cambridge, Massachusetts 02138	10. Work Unit No.: ---
	11. Contract or Grant No.: NAS1-13814
12. Sponsoring Agency Name and Address: NASA Langley Research Center Hampton, Virginia 23665	13. Type of Report and Period Covered: Contractor Report
	14. Sponsoring Agency Code: ---

15. Supplementary Notes

NASA Langley Technical Monitor: Herbert R. Henderson

16. Abstract

This report discusses measurements made of the reflection factors of asphalt, concrete, and sod at oblique angles of incidence.

Initial measurements were carried out in an anechoic chamber to eliminate the effects of wind and temperature gradients. These were followed by measurements made outdoors over a wider frequency range. Data are presented for the magnitudes of the reflection factors of asphalt, concrete, and sod at angles of incidence of 38° and 45°.

17. Key Words (Suggested by Author(s))	18. Distribution Statement
Ground Reflection, Ground Impedance, Reflection Factor	Unclassified

19. Security Classif. (of this report)	20. Security Classif. (of this page)	21. No. of Pages	22. Price*
Unclassified	Unclassified		

* For sale by the National Technical Information Service, Springfield, Virginia 22161

Page
Intentionally
Left Blank

TABLE OF CONTENTS

LIST OF FIGURES

SECTION 1

INTRODUCTION

In outdoor sound propagation problems, especially in outdoor acoustical testing, sound reflected from the ground contaminates in the direct sound to be measured. This contamination is basically unavoidable. Knowledge of the ground reflection factor is useful in:

(1) Predicting the possible extent of ground contamination in the planning stages of an experiment, and

(2) Reconstructing the direct sound from the measured sound, that is contaminated by the ground reflection.

This study was initiated to develop practical, workable methods by which the reflection factor of representative ground surfaces could be measured. Interest was centered upon surfaces commonly encountered in aeronautics, such as asphalt and sod (grass-covered soil).

Item (2) above, requires knowledge of the phase as well as the amplitude of the reflection factor. As a consequence, the first phase of this project was aimed at developing methods of measuring the phase as well as the amplitude of the reflection factor. A method had already been developed for measuring the amplitude of the reflection factor, one that was demonstrated to work on a specific, highly absorptive surface (Vér and Myles, 1973)*. The initial measurements were carried out in an anechoic chamber in order to eliminate the effects of wind and temperature gradients. In later phases of the program, outdoor measurements were conducted for the dual purposes of extending the frequency range of the data obtained indoors, and estimating, as far as possible, the effects of meteorological conditions near the ground.

---

*A list of references is provided on page 43.

SECTION 2

CORRELATION METHOD – HARMONIC INPUT SIGNAL

2.1 Description of Method

During the first phase of the program, an attempt was made to measure both the phase and the amplitude of the reflection facotr. The method used is described below.

A schematic drawing of the experimental set up is shown in Fig. 1. (The instrumentation used is discussed in Sec. 2.2.) The basic idea of the method was to create an omnidirectional sound field at the desired frequency, and to measure the correlation between the harmonic input signal supplied to the driver (sound source) and the output signal from the microphone. This measurement is made once with only the driver and microphone in the anechoic chamber, and then again with the test surface in place. In the first case, the microphone receives only the acoustic signal that travels directly from the driver, whereas in the second case both the direct signal and the signal reflected off the test surface are present.*

The electrical signal supplied to the driver is a simple sinusoid, which may be written as

$$e(t) = \mathrm{Re}\left\{ E e^{i\omega t} \right\} \qquad (1)$$

where "Re" is an abbreviation for "the real part of," and ω is the radian frequency of the signal. In a free field (no reflecting surface present), the sound pressure at a distance, s, from the driver may be written as

$$p_1(t) = \mathrm{Re}\left\{ EA \frac{e}{s}^{i\omega(t-s/c)} \right\} \qquad (2)$$

---

*If the surface being measured is highly absorptive, a barrier must be used in the chamber to attenuate the direct signal so that it is comparable in amplitude to the reflected signal. Three, rather than two sets of measurements are then required, but the essential features of the method are not altered. Refer to Ver and Myles (1973) for details.

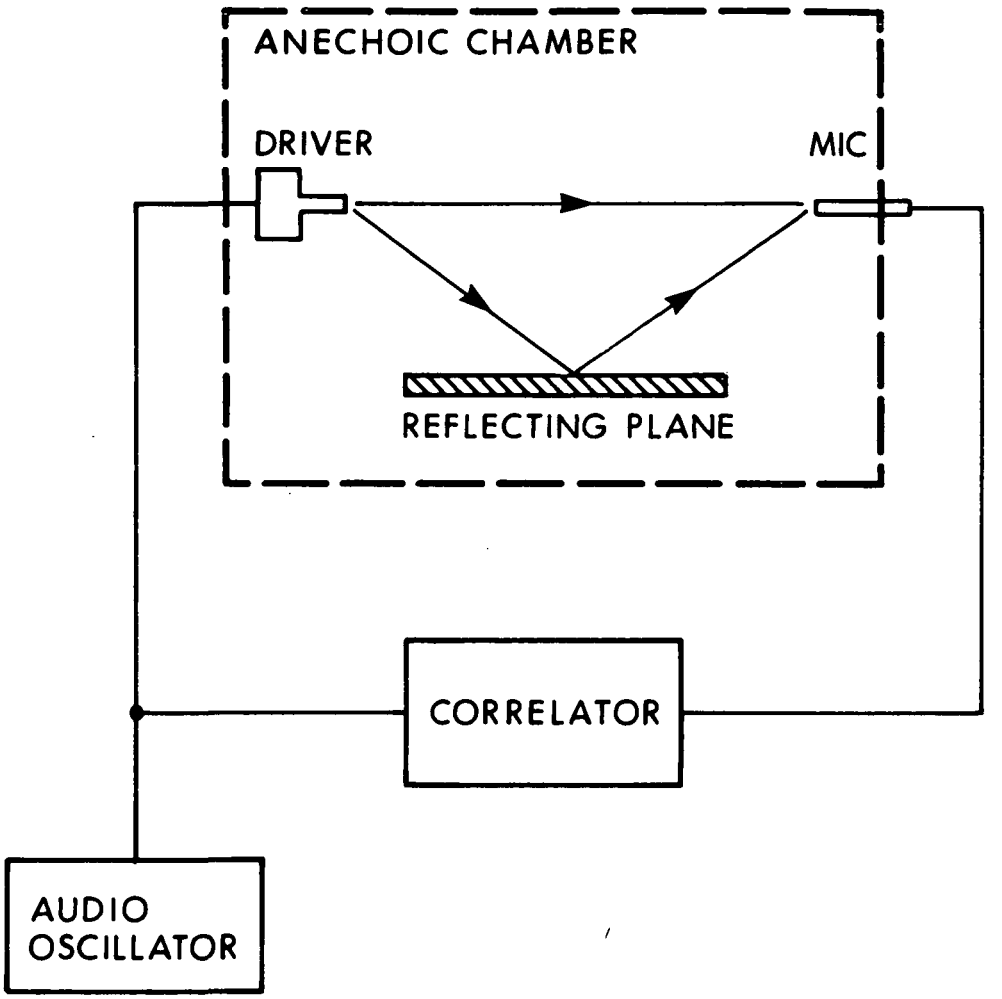

FIG. 1. SCHEMATIC OF SINE WAVE CORRELATION METHOD.

where A is a complex quantity representing the acoustic output of the driver at a unit distance, and c is the speed of sound.

With the reflecting plane in place, the pressure at the same straight-line distance, s, from the source is

$$p_2(t) = \mathrm{Re}\left\{ EA \left[\frac{e^{i\omega(t-s/c)}}{s} + R\,\frac{e^{i\omega(t-r/c)}}{r} \right] \right\} \qquad (3)$$

In this equation, R is the complex reflection factor of the surface under investigation, and r is the length of the reflected path (see Fig. 2).

As mentioned previously, the cross-correlation functions of the electrical input to the driver (Eq. 1) and the microphone response are measured first with only the driver and microphone in the chamber, and again with the reflecting plane in place. In the first case, the cross-correlation function, obtained from Eqs. (1) and (2), is

$$C_1(\tau) = |E|^2\,|A| \cdot \mathrm{Re}\left\{ \frac{e^{i\omega\left(\tau - \frac{s}{c} + \frac{\phi_A}{\omega}\right)}}{s} \right\} \qquad (4a)$$

while in the second case it is

$$C_2(\tau) = |E|^2\,|A| \cdot \mathrm{Re}\left\{ \frac{e^{i\omega\left(\tau - \frac{s}{c} + \frac{\phi_A}{\omega}\right)}}{r} + |R|\,\frac{e^{i\omega\left(\tau - \frac{r}{c} + \frac{\phi_A}{\omega} + \frac{\phi_R}{\omega}\right)}}{r} \right\} \qquad (4b)$$

In these equations, $|A|$ and ϕ_A are the modulus and phase of A, $|R|$ and ϕ_R are the modulus and phase of R, and τ is an arbitrary delay time. It is convenient to re-write these expressions as

$$C_1(\tau) = \mathrm{Re}\left\{ C_1 e^{i\omega(\tau - T_1)} \right\} \qquad (5a)$$

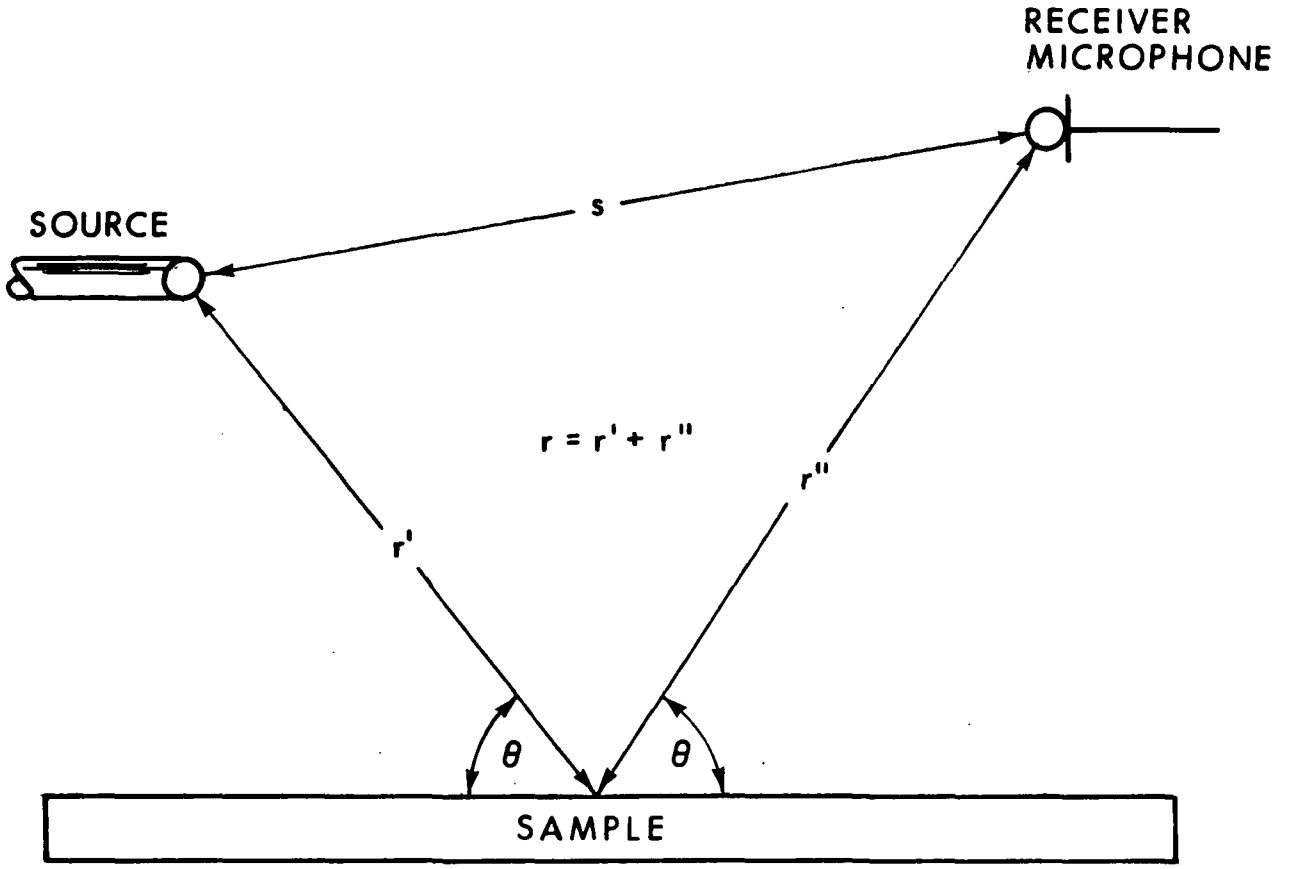

FIG. 2. GEOMETRY OF EXPERIMENT.

$$C_2(\tau) = \mathrm{Re}\left\{ C_1 e^{i\omega(\tau - T_1)} + C_r e^{i\omega(\tau - T_r)} \right\} \tag{5b}$$

where

$$C_1 \equiv \frac{|E|^2 |A|}{s} \tag{6a}$$

$$C_r \equiv \frac{|E|^2 |A| |R|}{r} \tag{6b}$$

$$\omega T_1 \equiv \frac{\omega s}{c} - \phi_A \tag{6c}$$

$$\omega T_r \equiv \frac{\omega r}{c} - \phi_A - \phi_R \tag{6d}$$

From Eqs. (6a through 6d), the amplitude and phase of the reflection factor can be solved for:

$$|R| = \frac{r C_r}{s C_1} \tag{7a}$$

$$\phi_R = \omega(T_1 - T_r) + \frac{\omega}{c}(r - s) \tag{7b}$$

However, in the experiment only the amplitudes and phase lags of the two correlation functions may be measured directly. The amplitude and phase lag of the free-field correlation function $C_1(\tau)$ are the quantities C_1 and ωT_1 appearing in Eq. (5a); the amplitude, C_2, and phase lag, ωT_2, of the correlation function, $C_2(\tau)$, satisfy the complex equation

$$C_2 e^{-i\omega T_2} = C_1 e^{-i\omega T_1} + C_r e^{-i\omega T_r} \tag{8}$$

which follows from Eq. (5b). C_r and T_r can be determined by solving this equation (which, being complex, is equivalent to *two* real equations). A phasor diagram of this equation is shown in Fig. 3. Once C_r and T_r are known, the amplitude and phase of the reflection factor can be obtained from Eqs. (7a) and (7b).

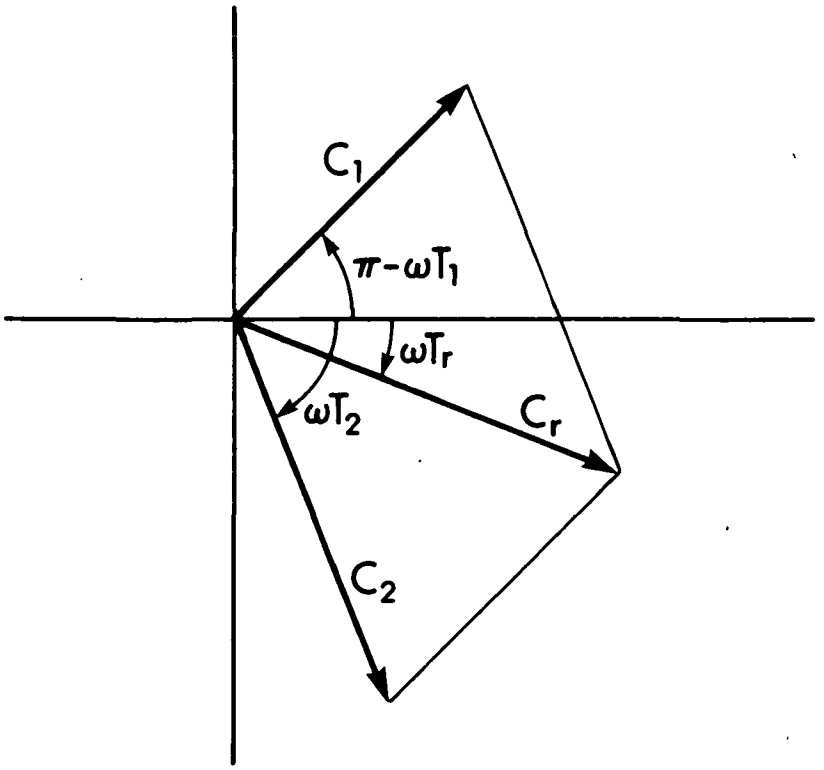

$$C_r e^{-i\omega T_r} = C_2 e^{-\omega T_2} - C_1 e^{-i\omega T_1}$$

FIG. 3. GRAPHICAL SOLUTION FOR AMPLITUDE AND PHASE OF REFLECTED WAVE (PHASOR DIAGRAM).

2.2 Instrumentation

The heart of the measurement system, as shown in Fig. 4, is a digital correlator in parallel with a phase meter. The source oscillator is tuned to a fixed freuqency, and the correlator and phase meter receive as inputs the output signal of the source amplifier and the microphone signal; the latter is filtered for better signal-to-noise ratio. The amplitude of the calculated correlation function (a sine wave) and the indicated phase angle serve as inputs into a computer program to evaluate Eqs. (7a) and (7b) for the amplitude and phase of the reflection factor.

Because a level difference between the direct and reflected path directions of even a few decibels could result in a significant error in computing the reflection factor, the sound source must be omnidirectional. The source arrangement used consisted of an electrostatic horn driver and an acoustic transmission line made up of flexible plastic tubing and ordinary 1/2 in. iron pipe. The driver, described in Vér and Myles (1973), remained outside the chamber. That portion of the pipe within the chamber was lagged to minimize spurious sound radiation. The pipe was terminated by a pipe "T" fitting oriented horizontally, as shown in Fig. 5. The source had a radiation pattern which was cylindrically symmetric about the axis of the "T", and so radiated equally in the directions of both the direct and reflected paths. Measurements made at several angles indicated that the source was indeed cylindrically non-directional to within ±1.0 dB. By plugging the openings of the "T", it was also established that the intensity of the sound radiated by the pipe walls was at least 28 dB lower than that of the sound radiated from the pipe termination at all frequencies of interest.

2.3 Discussion of Results

Results typical of those obtained by this method are shown in Fig. 6. The reflecting surface is an aluminum sheet 5/16 inch thick and about four feet square. The sheet was placed on glass fiber pads to minimize resonant oscillations. Also shown in the same figure is the magnitude of the reflection factor as determined by the phase cancellation method (Vér and Myles, 1973).

The two methods provide comparable values for the amplitude of the reflection factor except at low and high frequencies. More important is the behavior of the phase angle ϕ_R, which is

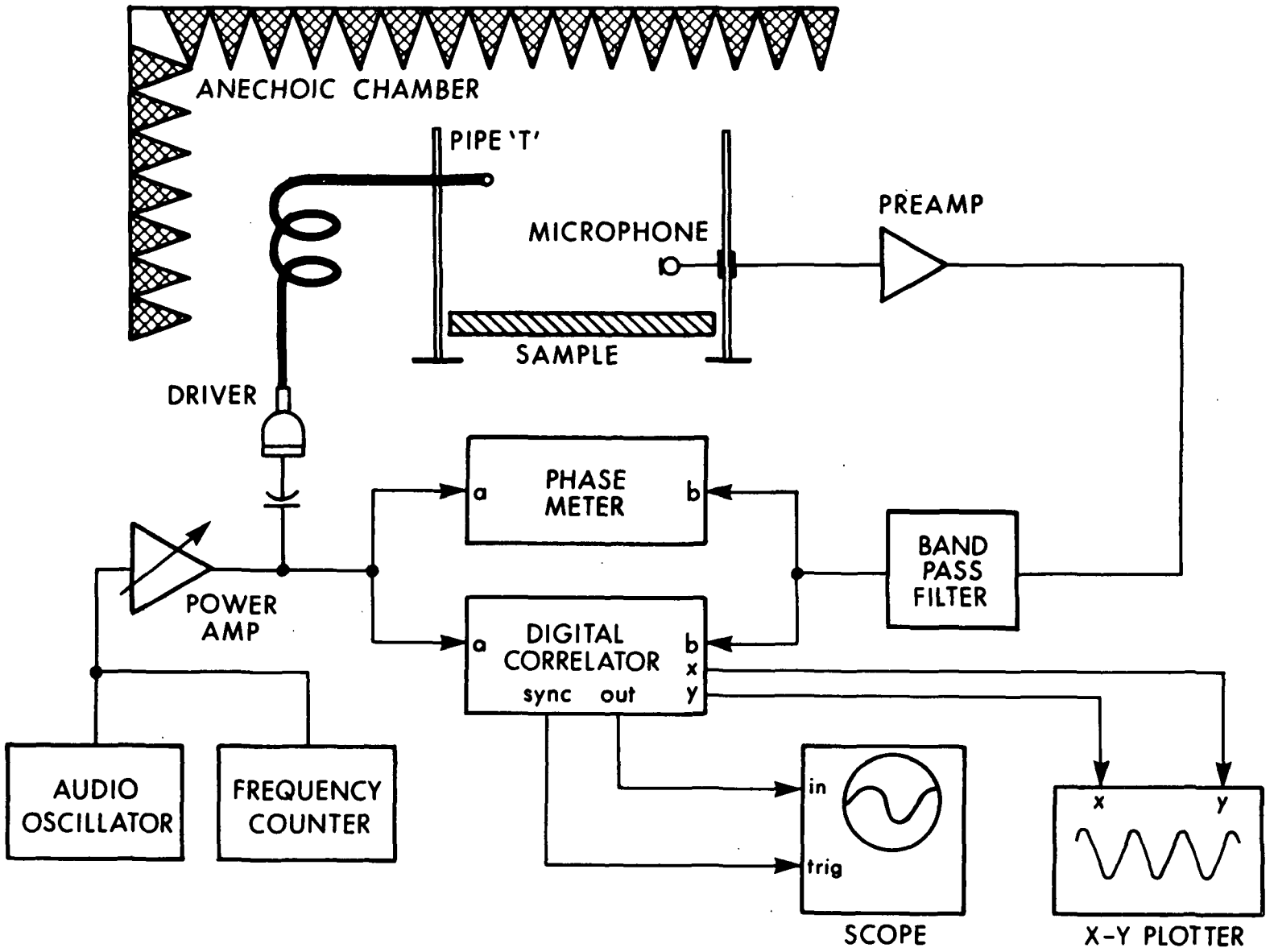

FIG. 4. INSTRUMENTATION BLOCK DIAGRAM; SINE WAVE CORRELATION METHOD.

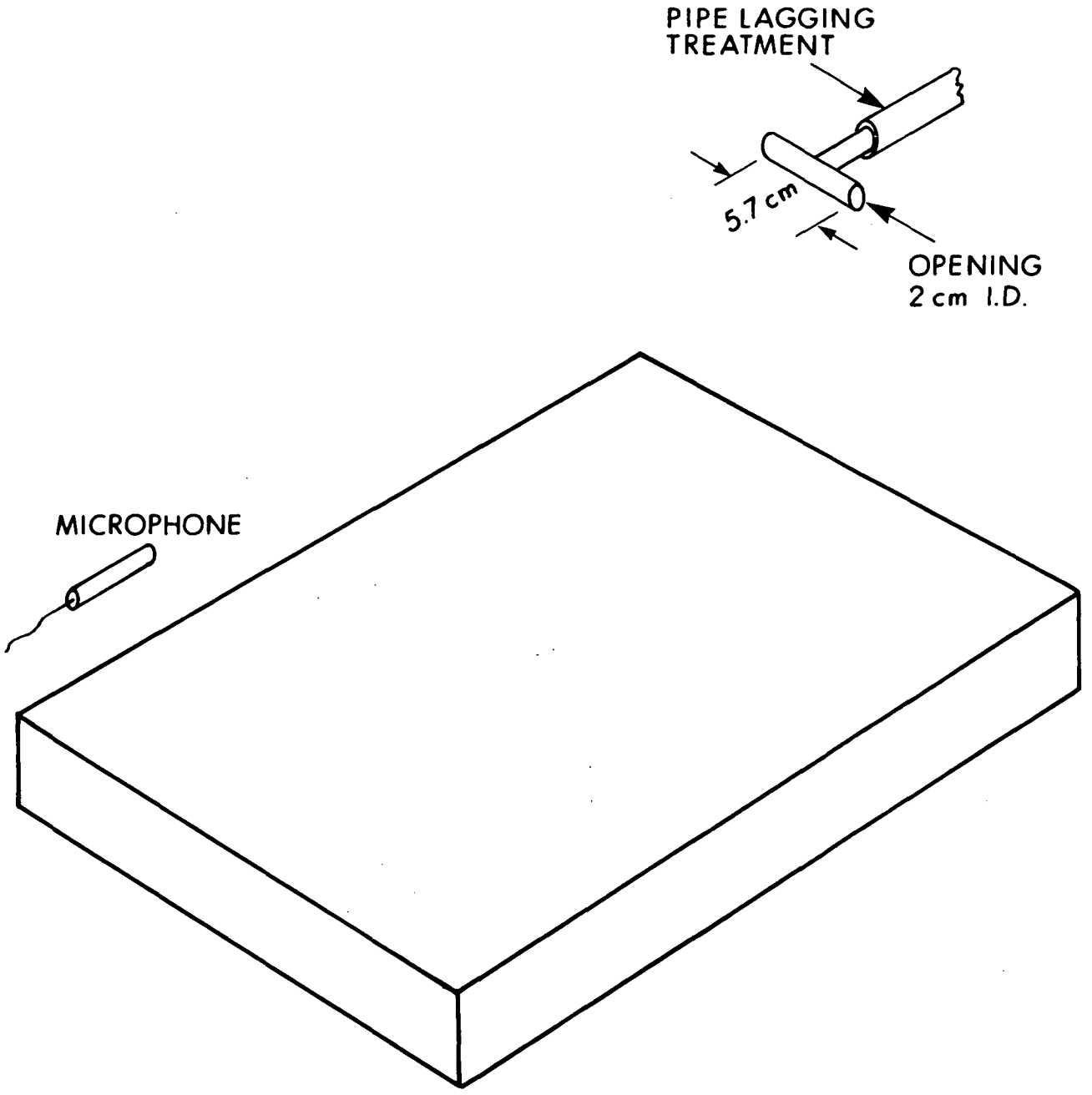

FIG. 5. SOUND SOURCE "T" TERMINATION.

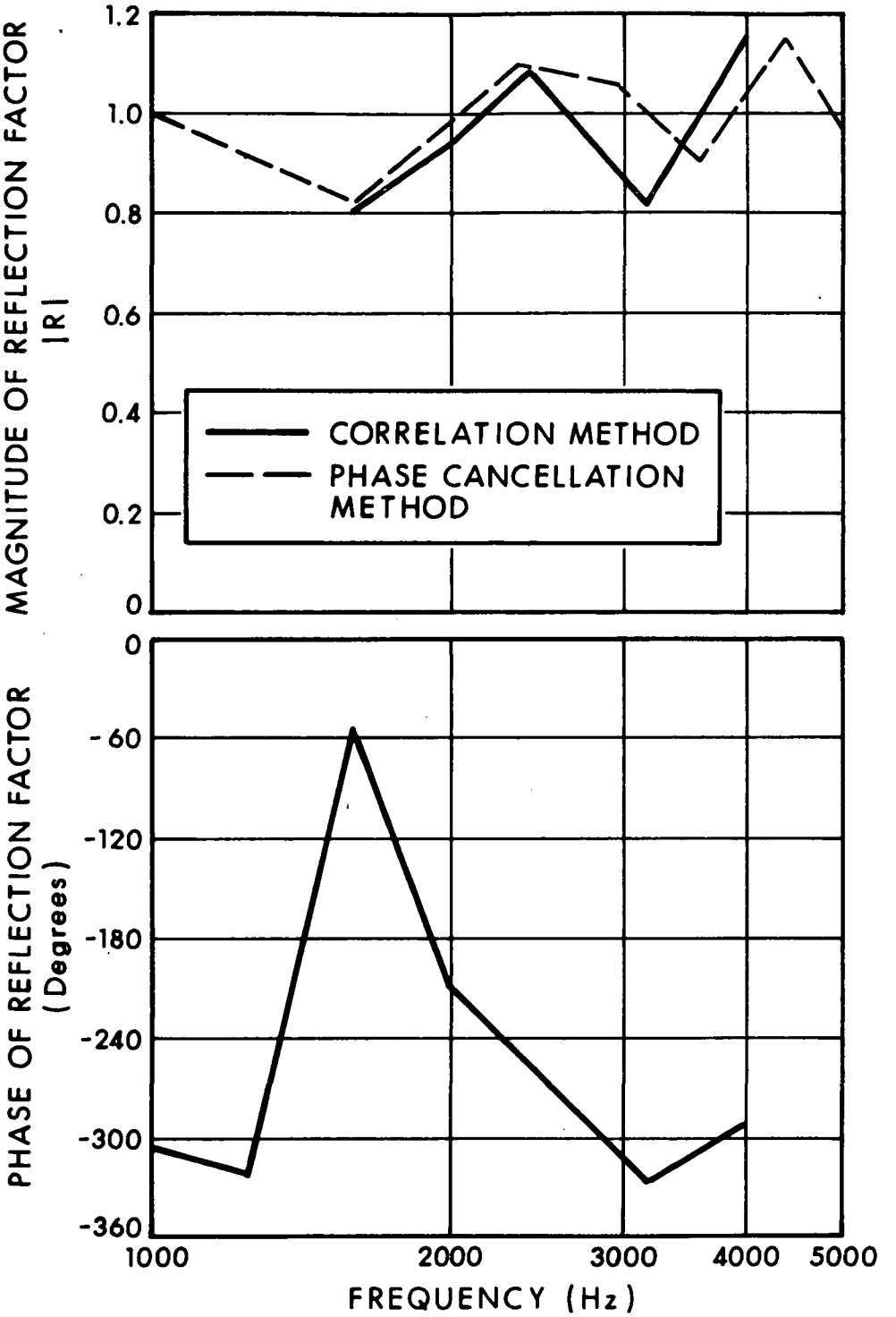

FIG. 6. MEASURED MAGNITUDE AND PHASE OF REFLECTION FACTOR; ALUMINUM PLATE, $\theta = 45°$.

not as expected. Because the aluminum plate is a hard surface, the phase angle should be small except near the coincidence frequency, which for this plate and angle of incidence is about 42000 Hz. When the experiment was repeated at the same reflection angle but with a slightly different relative placement of source, reflecting plane, and receiver microphone, the measured values of the magnitude of the reflection factor were found to be repeatable with a precision of ±10%. However, the measured values of the phase angle could not be repeated.

The phase angle ϕ_R is determined by comparing the phases of the direct and reflected signals. Refering to Eq. (7b), and noting that $\omega/c = 2\pi/\lambda$, ($\lambda \equiv$ wavelength),

$$\phi_R = 2\pi f (T_i - T_r) + 2\pi \left(\frac{r-s}{\lambda}\right) \tag{9}$$

Let Δ_{rs} be the error incurred in measuring the path length difference (r-s). The concommitant error in ϕ_R is

$$\frac{\Delta\phi_R}{2\pi} = \frac{\Delta_{rs}}{\lambda}$$

In this equation, the error $\Delta\phi_R$ has been normalized by 2π radians, or 360°. The allowable error in the path length measurement is related to the wavelength of the acoustic signal, rather than to the lengths of the propagation paths. This fact imposes a stringent requirement on the dimensional accuracy of the test arrangement, particularly at the high frequencies.

At lower frequencies, where this requirement is less severe, diffraction from the edges of the sample can contaminate the results. We sought to minimize this source of error by using samples whose lateral dimensions were 4 to 6 times the longest wavelengths involved, and by arranging the sound source, sample, and receiver microphone so that the acoustic image point was centered on the sample. (The image point is that point on the sample where a ray extending from the sound source to the sample and from there to the microphone forms equal angles, θ, of incidence and reflection.) Despite these precautions, spurious signals believed to be caused by edge diffraction were encountered at all frequencies (see Sec. 3.3).

Our inability to achieve repeatable results in the anechoic chamber using the correlation method led us to revert to the phase cancellation method for all subsequent indoor measurements.

SECTION 3

PHASE-CANCELLATION MEASUREMENTS

3.1 Review of Method

The phase-cancellation method (Vér and Myles, 1973) was used for all subsequent indoor measurements. With this method, the sound pressure level created by an omnidirectional point source in an empty anechoic chamber was recorded on a strip chart as the frequency was varied. These measurements were repeated with the sample reflecting surface in place (recorded, for convenience, on the same strip chart). The second trace displays pronounced maxima and minima at those frequencies for which the direct and reflected acoustic signals interfered constructively and destructively. By comparing the sound levels recorded with and without the sample in place, the magnitude of the reflection factor can be inferred. In principle, the frequencies at which the constructive or destructive interference occurs can be used to determine the phase angle of the reflection factor as well. However, our measurements of the phase angle displayed the same scatter as encountered in the sine wave correlation measurements discussed in Section 2. This scatter can be attributed to diffraction from the edges of the sample (see Section 3.2).

Referring to Fig. 2 and Eq. (3), the pressure at the receiver microphone at a frequency for which destructive interference (pressure minimum) occurs is

$$|P_{min}| = |EA| \left(\frac{1}{s} - \frac{|R|}{r} \right) \tag{10}$$

while at a frequency at which constructive interference (pressure maximum) occurs,

$$|P_{max}| = |EA| \left(\frac{1}{s} + \frac{|R|}{r} \right) \tag{11}$$

In the absence of the sample, the pressure is given by the first term in each of these expressions:

$$|P_{free}| = \frac{|EA|}{s} \tag{12}$$

The ratios of the pressure minima and maxima to the free-field levels at the same frequency can be used to determine the reflection coefficient (amplitude of the reflection factor) at the respective frequencies. Specifically, at a frequency for which destructive interference occurs,

$$|R| = \frac{r}{s}\left(1 - |P_{min}/P_{free}|\right) \tag{13}$$

while at a frequency for which constructive interference occurs,

$$|R| = \frac{r}{s}\left(|P_{max}/P_{free}| - 1\right) \tag{14}$$

Two sources of error inherent in this method of measurement must be mentioned. First, if the free field pressure (P_{free} in Eqs. [13] and [14] above) varies rapidly with frequency, it is difficult to judge precisely the extreme values of the pressure ratios by inspecting the strip chart recording (a sample of which is shown in Fig. 8). In our experiments, this variation was reduced by using a feedback arrangement to minimize the variation of the free field output of the sound source with frequency (see Section 3.2). Second, when destructive interference occurs, the sound pressure levels being measured may be quite small. For example, at a grazing angle of incidence of 30°, and in a situation where the source and receiver are equidistant from the surface, the ratio of direct to reflected path lengths is $s/r = \cos(30°) = 0.866$. If the surface is very hard so that $|R| \doteq 1$, then, from Eqs. (10) and (12)

$$P_{min}/P_{free} = \left(1 - \frac{s}{r}\,|R|\right) = 0.134 \tag{15}$$

In this case, the minimum pressure is about 17 dB lower than the free field value. The background noise level, as well as extraneous emissions from the point source (casing radiation or harmonics of the driver frequency) must be reduced to at least 10 dB below this level, or 27 dB below the free-field level. This places stringent requirements upon both the performance characteristics of the noise source, and the environment in which the measurements are made. These requirements are more severe for highly reflective surfaces and for grazing angles of incidence (which correspond to $R \doteq 1$ and $s/r \doteq 1$ in Eq. [15]).

3.2 Instrumentation

The phase cancellation method, which is essentially the same as that described by Vér and Myles (1973), employs a swept oscillator/tracking filter arrangement, as shown in Fig. 7.

The omnidirectional source exposes the sample to a pure tone acoustic signal generated by an oscillator whose frequency is varied continuously. The tracking narrow band filter, ganged to the oscillator, is always centered on the frequency of the swept sine wave and filters the output from the measurement microphone. The filtered microphone output level is recorded as a function of frequency on the graphic level recorded. Two frequency sweeps are made, one with the sample surface in the chamber, and one with the chamber empty. A sample recording is shown in Fig. 8.

As mentioned previously, a refinement was made in the technique which reduced the measurement error caused by the non-flat frequency response of the source. An automatic level recorder, or compressor, was used to regulate the output of the sound source as the frequency of the oscillator was swept upward. The controlling feedback was provided by a microphone placed near to the source. In order to eliminate low frequency ambient noise that would have disturbed the feedback signal, the control microphone output was A-weighted before the control input of the compressor. As a result of this level regulation procedure, the on-axis response of the source-receiver system was nearly flat with frequency, so that the difference between the two graphic level recorder traces could be read directly, without the errors introduced by variations in the frequency response $A(\omega)$.

The BBN anechoic chamber in which these measurements were made is 2.4 m high and has a floor measuring about 2.4 m by 3 m. The lower cut-off frequency of the chamber is about 400 Hz.

The floor of the chamber is constructed of wire mesh. In order to preserve the dimensional integrity of the experiment with workers moving about in the chamber, the pipe that formed the point noise source was cantilevered from one wall, while the sample reflecting surfaces and the receiver microphone were suspended from the ceiling. The samples themselves consisted of plywood trays 7.5 cm deep and 1.22 m square, into which the concrete, asphalt, etc. were poured. The asphalt was heated with a blow torch and tamped down to compact it.

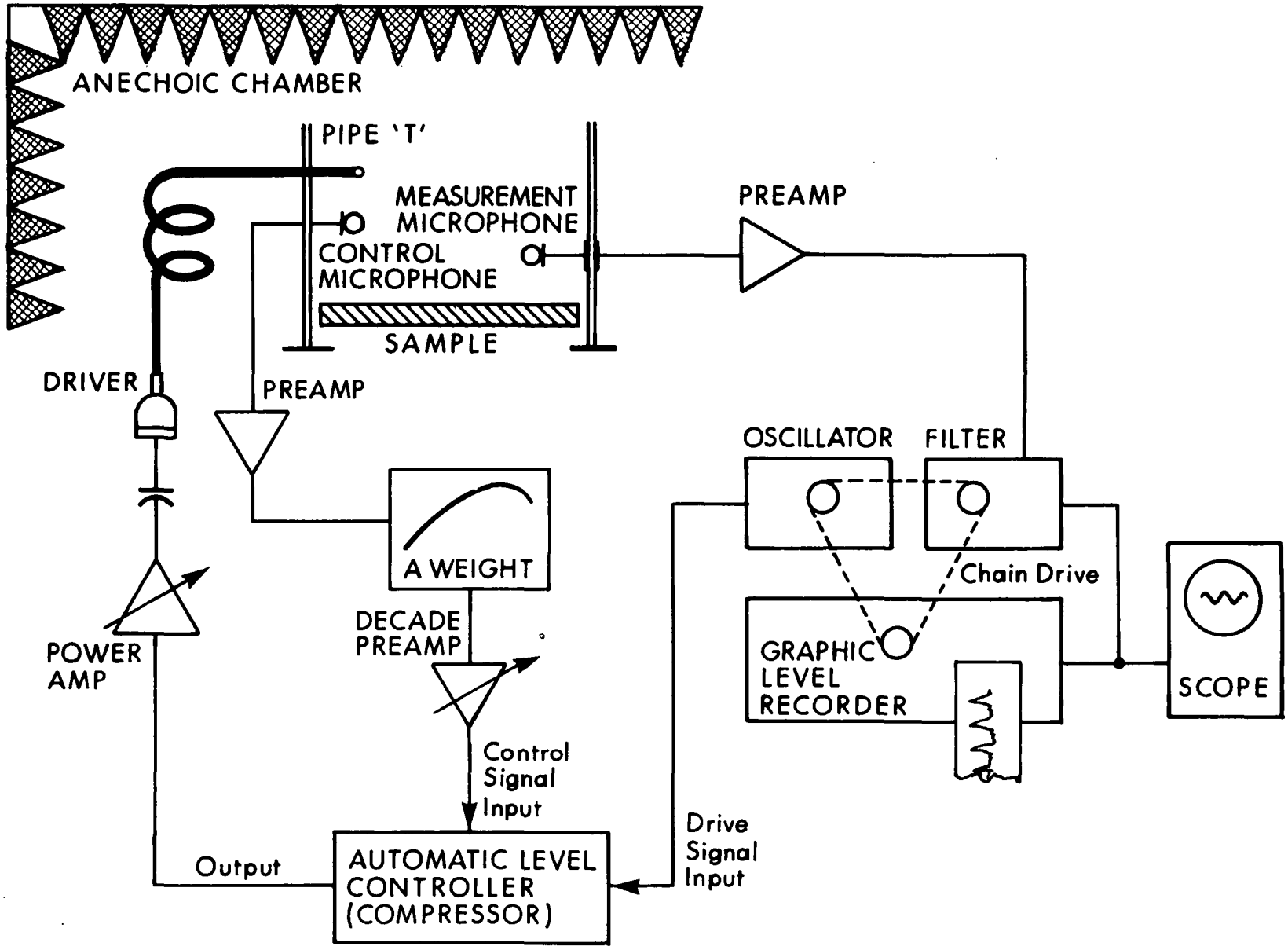

FIG. 7. INSTRUMENTATION BLOCK DIAGRAM; PHASE CANCELLATION METHOD.

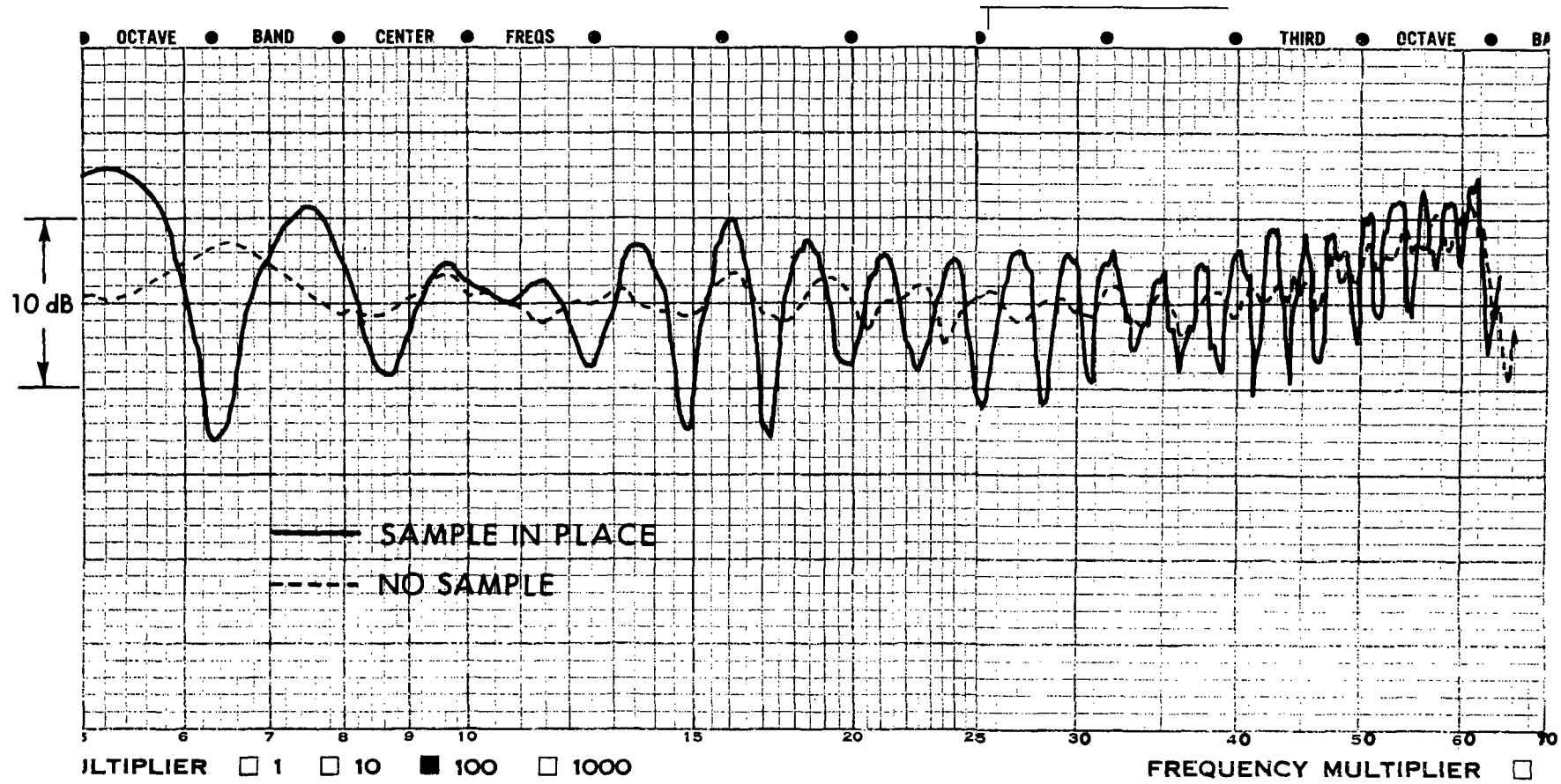

FIG. 8. TYPICAL STRIP CHART RECORDING; ASPHALT SAMPLE.

The 1.22 m square samples were the largest reflecting surfaces that could be accommodated within the chamber. It was not anticipated therefore, that meaningful measurements of the reflection factor could be made much below 1000 Hz. The actual limit turned out to be higher than this – about 2000 to 3000 Hz.

3.3 Results Obtained and Discussion

The strip chart recording diplayed in Fig. 8 is typical of the results obtained. In this case, the reflecting surface was asphalt; the sound source and receiver microphone were both elevated 123.2 cm above the surface, and were spaced 150.3 cm apart. The length of the direct path was 150.3 cm while the reflected path length was 288.3 cm.

The frequency increment between successive maxima or minima can be found by taking the absolute value of both sides of Eq. (3), and introducing $R = |R|\, e^{i\phi_R}$:

$$|p| = \frac{|EA|}{s} \left| 1 + \frac{s}{r} |R| \; e^{-i\left[\frac{\omega}{c}(r-s) - \phi_R\right]} \right|$$

The pressure maxima occur when

$$\frac{\omega}{c}(r-s) - \phi_R = 0,\ 2\pi,\ 4\pi,\ \ldots$$

and the minima when

$$\frac{\omega}{c}(r-s) - \phi_R = \pi,\ 3\pi,\ 5\pi,\ \ldots$$

The frequency increment between successive maxima (or minima) is then (assuming that the phase of the reflection factor ϕ_R, does not vary too rapidly with frequency),

$$2\pi \frac{\Delta f}{c} (r-s) = 2\pi$$

or

$$\Delta f = \frac{c}{r-s}$$

Using c = 342 m/sec and r-s = 288.3 - 150.3 = 138 cm, we obtain Δf = 247 Hz, which agrees reasonably well with the spacing between the extremes shown in Fig. 8.

However, the envelope of the solid line in the figure (measured with the asphalt sample in place) is itself modulated. The modulation is more pronounced at low frequencies, and the interval between the peaks in the modulation envelope is between 1200 and 1300 Hz.

One way to explain this modulation is to assume that sound diffracted from the edges of the sample nearest the sound source and receiver microphone interfered with the direct and reflected fields (see Fig. 9). Because of the symmetry of the locations of the noise source and receiver microphone, the lengths of the two diffracted paths are equal. In this situation the magnitude of the pressure at the microphone would be

$$|P| = |EA| \left| \frac{e^{-\frac{i\omega s}{c}}}{s} + R\,\frac{e^{-\frac{i\omega r}{c}}}{r} + De^{-\frac{i\omega d}{c}} \right| \qquad (16)$$

In this equation, d is the path length from the source to either of the fore and aft edges, and from there to the receiver microphone. D is the complex amplitude of the diffracted signal. The most pronounced maxima and minima will occur when the last two terms in Eq. (16) agree in phase, while the weakest will occur when they are out of phase. When they are in phase,

$$\frac{\omega}{c}(d-r) = 0,\ 2\pi,\ 4\pi,\ \ldots$$

while when they are out of phase,

$$\frac{\omega}{c}(d-r) = \pi,\ 3\pi,\ 5\pi,\ \ldots$$

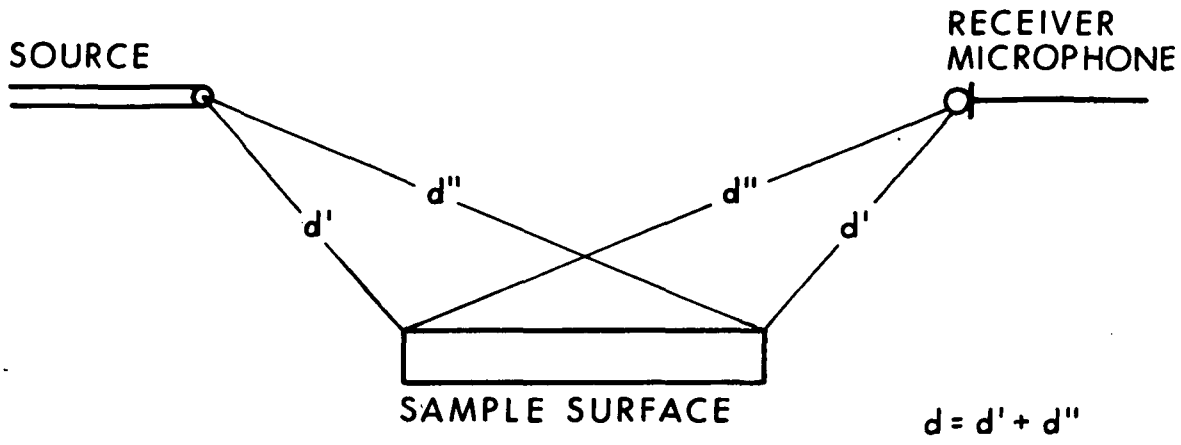

FIG. 9. TEST GEOMETRY, SHOWING DIFFRACTED RAY PATHS.

The frequency increment between any two successive phase additions or cancellations is

$$2\pi \frac{\Delta f}{c} (d-r) = 2\pi$$

so that

$$\Delta f = \frac{c}{(d-r)}$$

In the situation being discussed here, the distance d (to *either* edge) is 314.6 cm while r is 288.3 cm. Using c = 342 m/sec, we get

$$\Delta f = 1303 \text{ Hz} \quad ,$$

which agrees well with the period of the modulation in Fig. 8.

Once the importance of edge diffraction was realized, an attempt was made to diminish it by supporting two layers of 1/2 in. thick glass fiber mat above the edges of the sample so as to break the line of sight between source, edge, and receiver microphone. This reduced the amplitude of the modulation about 50% above 3000 Hz, but had little effect at lower frequencies.

Edge diffraction remains, therefore, a major limitation on the precision that could be realized in the indoor measurements of the reflection coefficient. This limitation applies as well to the sine wave correlation measurements discussed in Section 2.

The reflection coefficients (magnitude of the reflection factor) measured for concrete and asphalt are displayed in Figs. 10 and 11, respectively. Most of the scatter in the data, as well as the measured reflection coefficients exceeding unity in Fig. 10, may be attributed to edge diffraction, as discussed above. No results are shown for frequencies less than 2000 Hz for the same reason. The driver was unable to attain an adequate signal-to-noise ratio above 7000 Hz. Despite the spread in the data, the measured reflection coefficients for the asphalt sample are significantly lower than those for the concrete.

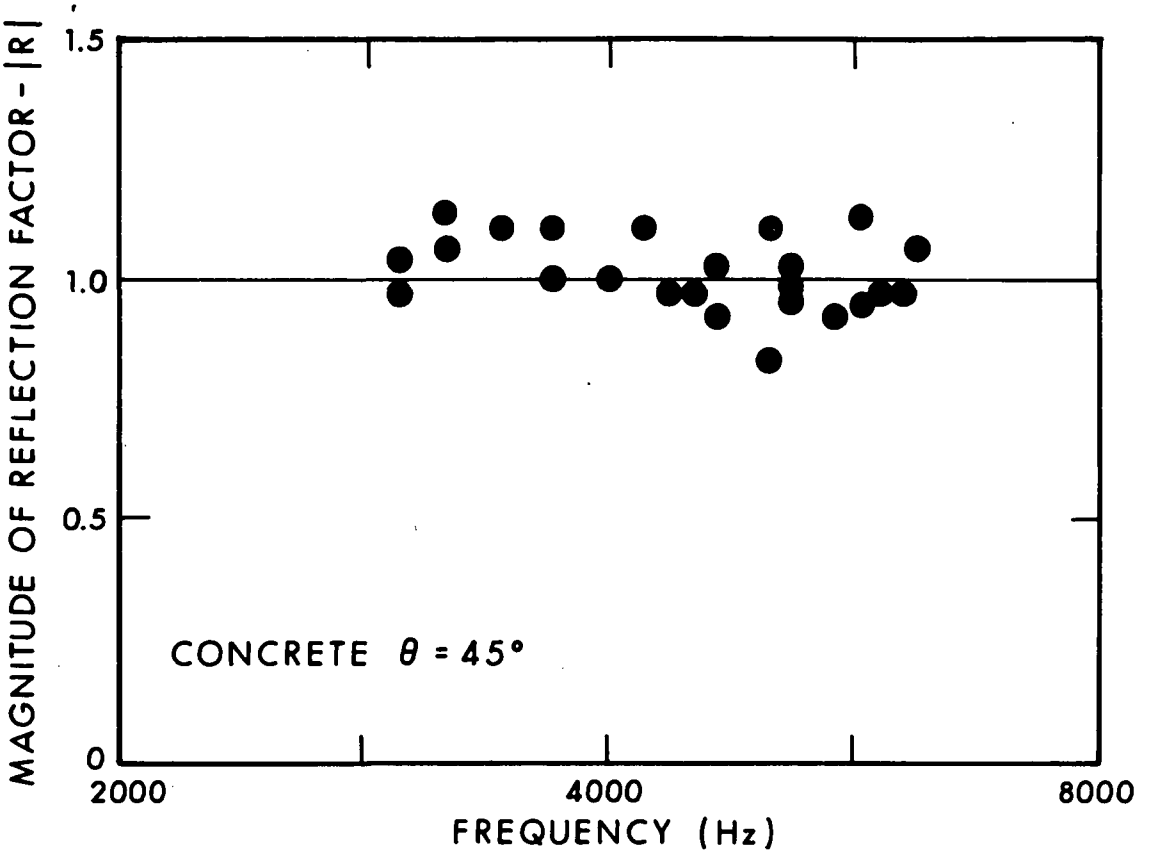

FIG. 10. REFLECTION COEFFICIENT; CONCRETE, θ = 45°.

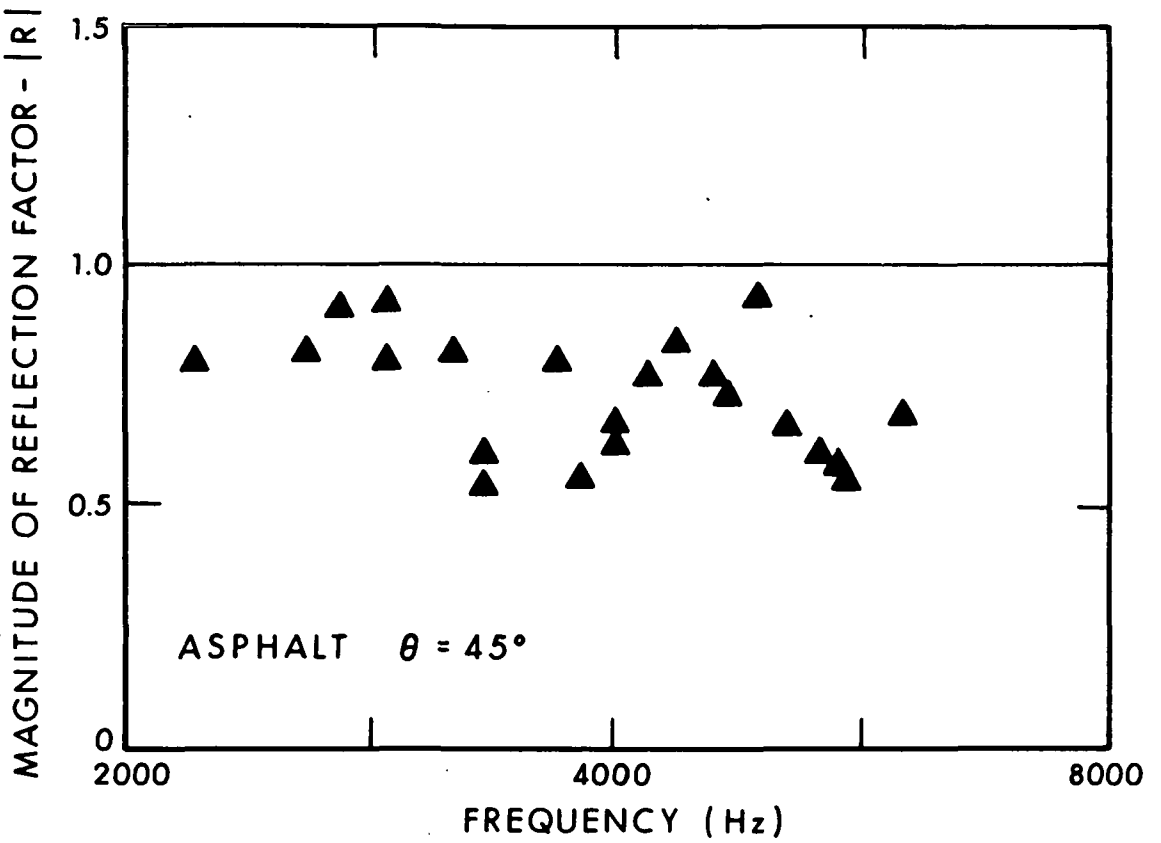

FIG. 11. REFLECTION COEFFICIENT; ASPHALT, θ = 45°.

Becuase of the limitations of the data obtained in the anechoic chamber for asphalt and concrete, no further indoor measurements were carried out. All subsequent tests were conducted outdoors.

SECTION 4

FILTERED RANDOM NOISE CORRELATION METHOD; OUTDOOR MEASUREMENTS

This method, which was employed to measure the reflection coefficient outdoors, avoids the gross sensitivity to geometry inherent in the sine wave correlation method, and the sensitivity to ambient noise that exists with the sine wave phase cancellation technique. It cannot, however, be used to measure the phase of the reflection factor.

4.1 Measurement Technique

The geometry of the experimental setup is the same as that depicted in Fig. 2. In this case, the source is fed with band limited random noise, whose Power Spectral Density is given by

$$G(\omega) = G \quad ; \quad \omega_\ell \leq \omega \leq \omega_u$$

$$= 0 \quad ; \quad \text{otherwise} \qquad (17)$$

$\omega_\ell \equiv$ band lower limit, $\omega_u \equiv$ band upper limit.

A "source microphone" is placed close to the source, the output of which is correlated with the signal measured at the receiver microphone position. Using the nomenclature presented previously, the cross-correlation function is thus

$$C(\tau) = \frac{1}{2\pi} \int_{-\infty}^{\infty} \left\{ \frac{G(\omega)\, e^{i\omega\left(\tau - \frac{s-s_1}{c}\right)}}{ss_1} + \frac{G(\omega)R(\omega)\, e^{i\omega\left(\tau - \frac{r-s_1}{c}\right)}}{sr} \right\} e^{i\omega\tau}\, d\omega \qquad (18)$$

where $s_1 \equiv$ distance from source to source microphone.

We assume that $R(\omega)$ is constant over the frequency band and represent it as $|R|\, e^{i\phi_R}$. By noting that we can change the limits of integration to those of the passband and that G is constant over the band, we obtain:

$$C(\tau) = \frac{1}{2\pi} \int_{\omega_\ell}^{\omega_u} \left\{ \frac{G\, e^{i\omega\left(\tau - \frac{s-s_1}{c}\right)}}{ss_1} + \frac{G|R|\, e^{\left[i\omega\left(\tau - \frac{r-s_1}{c}\right) + i\,\phi_R\right]}}{rs_1} \right\} e^{i\omega\tau}\, d\omega \qquad (19)$$

By defining $\xi = t + \frac{s_1}{c}$; we obtain

$$C(\xi) = \frac{1}{\pi} \int_{\omega_\ell}^{\omega_u} \left\{ \frac{G \cos\left[\omega\left(\xi - \frac{s}{c}\right)\right]}{ss_1} + \frac{G|R| \cos\left[\omega\left(\xi - \frac{r}{c}\right)\right]}{rs_1} \right\} d\omega \qquad (20)$$

For convenience, we define $\Delta\omega = \omega_u - \omega_\ell$ and $\omega_c = \frac{\omega_\ell + \omega_u}{2}$. Thus,

$$C(\xi) = \frac{2}{\pi} \left\{ \frac{G \sin\Delta\omega\left(\xi - \frac{s}{c}\right)}{ss_1\left(\xi - \frac{s}{c}\right)} \cos\omega_c\left(\xi - \frac{s}{c}\right) + \frac{G|R| \sin\Delta\omega\left(\xi - \frac{r}{c}\right)}{rs_1\left(\xi - \frac{r}{c}\right)} \cos\omega_c\left(\xi - \frac{r}{c} + \phi_R\right) \right\} \Delta\omega \qquad (21)$$

This function consists of two sin x/x envelopes centered at times $\xi_1 \equiv \xi - s/c$ and $\xi_2 \equiv \xi - r/c$, with corresponding amplitudes, G/ss_1 and $G|R|/rs_1^2$.

We can see, by inspection, that the first envelope has coefficients related only to the direct path, and the second has coefficients related only to the reflected path. The reflection coefficient is thus obtained by the ratio of the magnitudes of the maxima of the two envelopes. Hence,

$$|R| = \frac{r}{s} \frac{C_2}{C_1} \tag{22}$$

where

$C_1 \equiv \frac{G}{ss_1}$; the measured magnitude of the maximum of the first envelope

$C_2 \equiv \frac{G|R|}{rs_1}$; the measured magnitude of the maximum of the second envelope

Note that Eq. (22) is valid only when the two envelopes are separated widely enough in time that the respective maxima are practically determined only by that sin x/x envelope which is centered at the specific time delay.

The argument of the envelope of the function in Eq. (21), is proportional to the signal bandwidth $\Delta\omega$. Consequently, the narrower the bandwidth, the broader the envelopes will be in delay time, and the greater the path length difference that must exist to avoid superposition of the two. This requirement creates an inverse relationship between frequency resolution and the physical size of the experiment. This situation is most acute for near-grazing incidence and low frequency bands (if proportional bandwidths, such as octave or one-third octave bandwidths, are used).

We found that a relative bandwidth of one octave represented a reasonable compromise solution to the size-frequency dilemma for the angles and frequencies we wished to measure. We were able to measure down to the 250 Hz octave band at an incidence angle of 45° with source-receiver separations of about 10 m.

(Our primary physical limitation was the height at which we could support the 10 kg driver, using a structure that was easy to erect and transport.)

Using a band of frequencies rather than a single tone gives a reflection factor averaged over the band. However, measurements made using single-frequency techniques (such as by Embleton, *et al.*, 1976) indicate that the reflection factor magnitudes for grass and asphalt are *not* strong functions of frequency, and so fine frequency resolution may not be a significant advantage. Moreover, measuring octave-band average reflection coefficients using the filtered white noise correlation technique is compatible with established methods of measuring acoustic absorption, notably the Reverberation Room Method (ASTM Standard C423 [1972]).

Lack of severe sensitivity to ambient noise, distance measurement errors, and phase made the filtered while noise correlation technique the most attractive for outdoor measurements, where conditions are much less controllable than in the laboratory. The results obtained using this technique were decidedly more consistent and repeatable than were data obtained using the methods described earlier.

The insensitivity of this method to ambient noise stems from the use of the cross-correlation function, which "ignores" extraneous noise that is not correlated with the source signal. This insensitivity to ambient noise is a distinct advantage, because finding suitable measurement sites at very quiet locations is often difficult. The technique can therefore be used when the reflection coefficient must be measured at a specific location where a high ambient noise is unavoidable.

The technique is insensitive to phase disturbances because the calculation of the reflection factor has no phase term. This, too, is indeed a great advantage for outdoor measurements because the need for precision distance measuring devices and time consuming procedure is eliminated, as are measurement ambiguities — e.g., to what depth of a layer of grass should the source-to-ground measurement be made? The only geometric function is the need for adequate path length differences, as discussed above.

Thus, although the technique cannot be used to measure the phase of the reflection factor, the simplicity of the setup, the ease with which the measurements are made, and the accuracy of the method make it a useful procedure.

4.2 Instrumentation

Figure 12 is a block diagram of the system as it was employed in the field. As with the sine wave correlation method, a digital correlator was the heart of the system. Both the noise source and the receiver microphone signals were filtered in a bandwidth of one octave using a tunable filter that could be centered at any arbitrary frequency (i.e., not only at standard octave band frequencies).

A special horn with a cylindrically symmetric radiation pattern, was fitted on the source driver. As seen in the photograph of Fig. 13, the horn is an exponential flare of revolution; i.e., it is a cylinder, any radial section of which is a horn-shaped flare.

Figure 14 shows a typical correlation plot. Two distinct sin x/x envelopes are visible; the one on the left corresponds to the direct path, while the one on the right corresponds to the reflected path.

4.3 Discussion of Results

The results of the outdoor measurements using the filtered white noise correlation technique are graphed in Figs. 15 through 18. These data are for the reflection factor averaged over a bandwidth of one octave centered at the frequency indicated. The method was used to measure the magnitude of the reflection factor for mowed grass and asphalt, at two angles of incidence for each surface.

The data were, in almost all cases, consistently repeatable to within the limits of experimental accuracy. At frequencies where repeat measurements were made, more than one measurement value is plotted in the graphs.

The data for grass (Figs. 15 and 16) gave a reflection factor well below 1.0 at all frequencies. The indicated trend of decreasing reflection (increasing absorption) with increasing frequency is to be expected, as wavelengths become smaller and approach the length of the blades of grass.

The asphalt data (Figs. 17 and 18) are consistently near 1.0 for all frequencies, as expected for a hard surface. Note that the 45° asphalt data agrees quite well with that measured with the phase cancellation method (see Fig. 11). The reflection coefficient at 45° decreased slightly with increasing

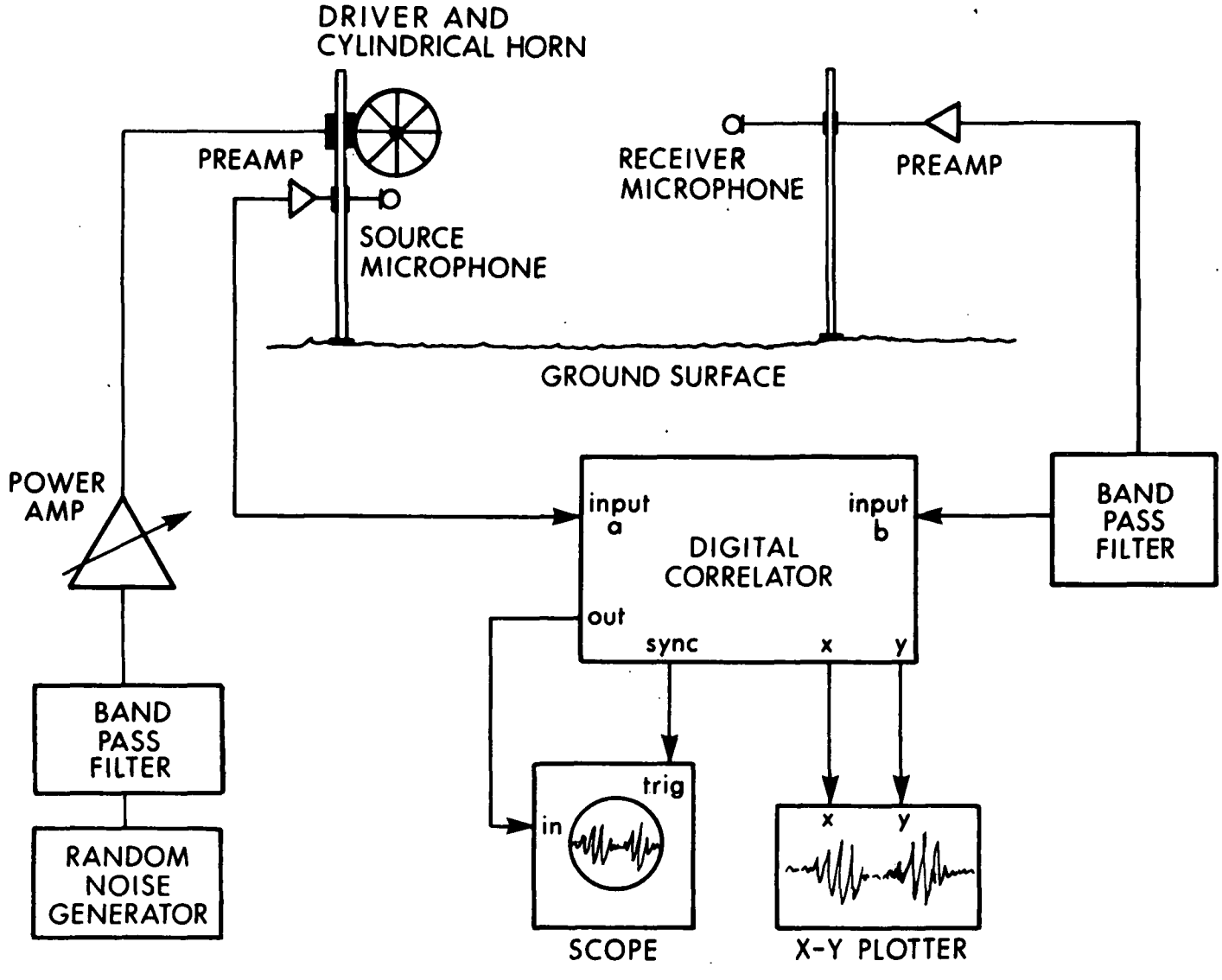

FIG. 12. INSTRUMENTATION BLOCK DIAGRAM; FILTERED WHITE NOISE CORRELATION METHOD.

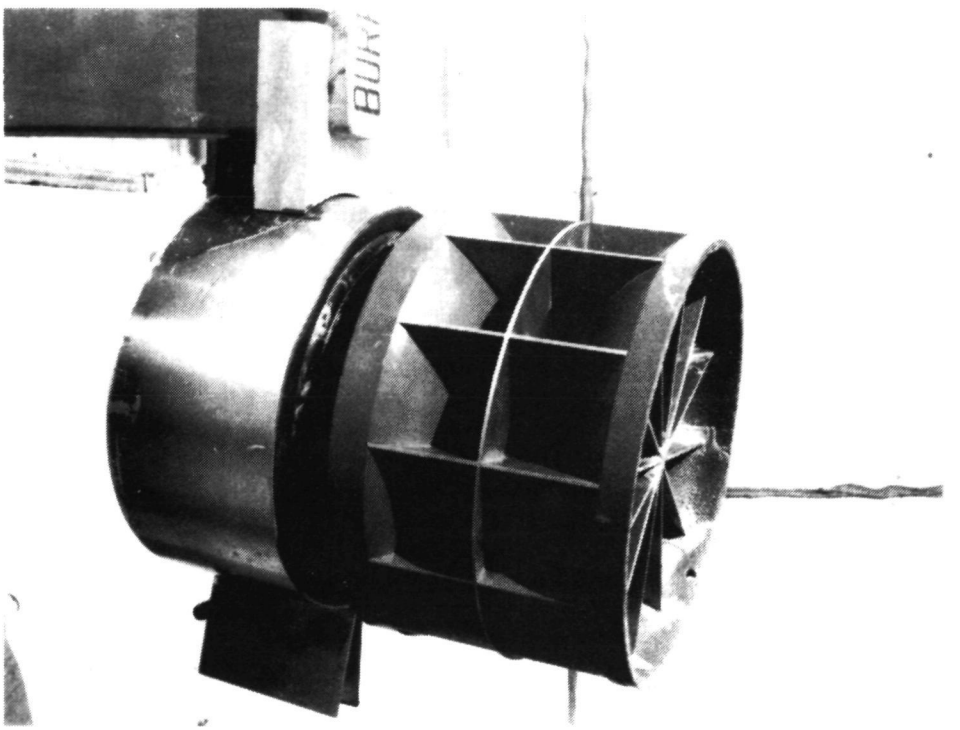

FIG. 13. PHOTOGRAPH OF CYLINDRICAL HORN FITTED TO SOURCE DRIVER.

FIG. 14. EXAMPLE OF CORRELATION PLOT: FREQUENCY = 2000 Hz, θ = 45° CALCULATED $|R|$ = 0.842, ASPHALT.

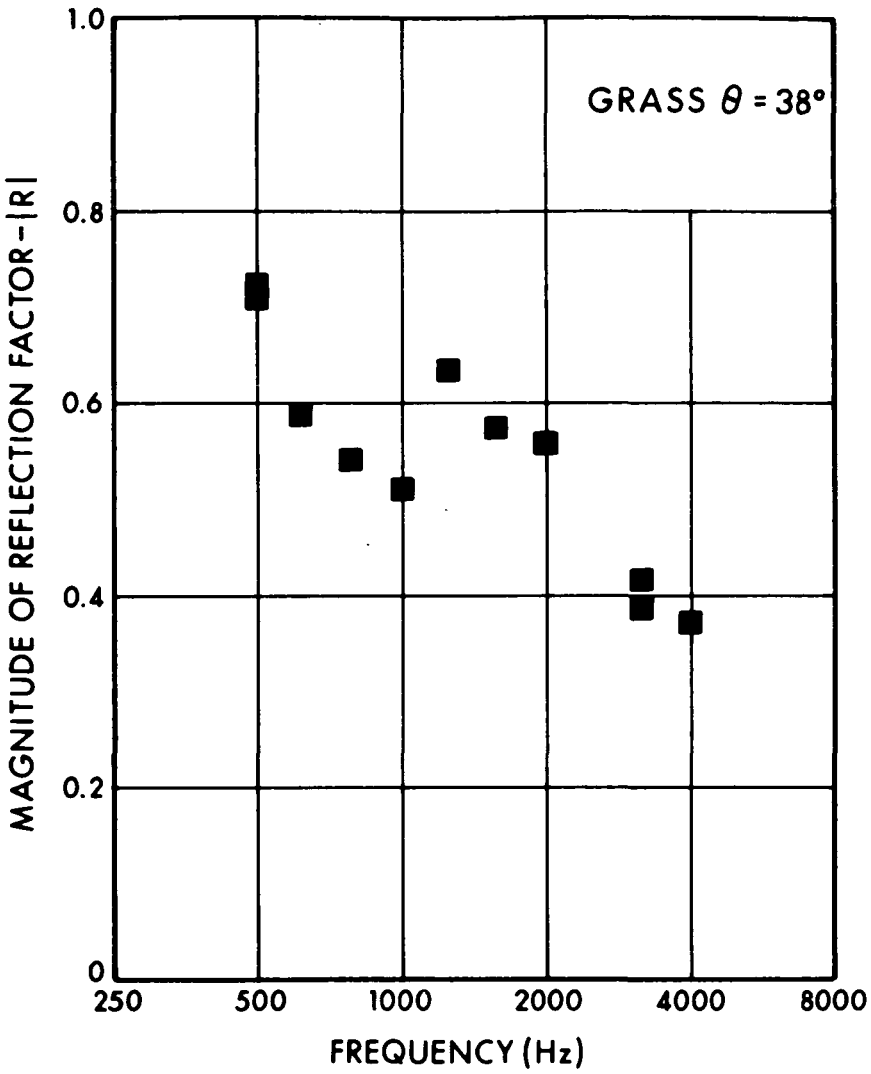

FIG. 15. REFLECTION COEFFICIENT; MOWED GRASS, θ = 38°.

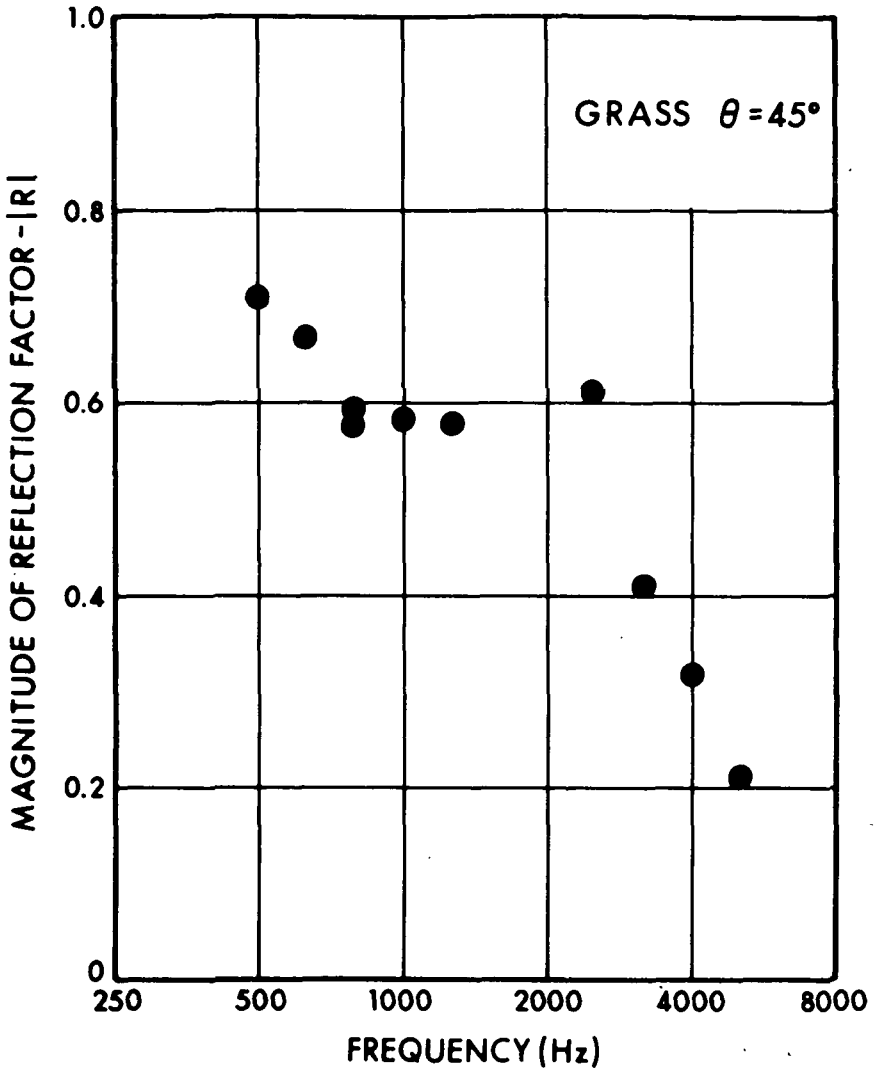

FIG. 16. REFLECTION COEFFICIENT; MOWED GRASS, θ = 45°.

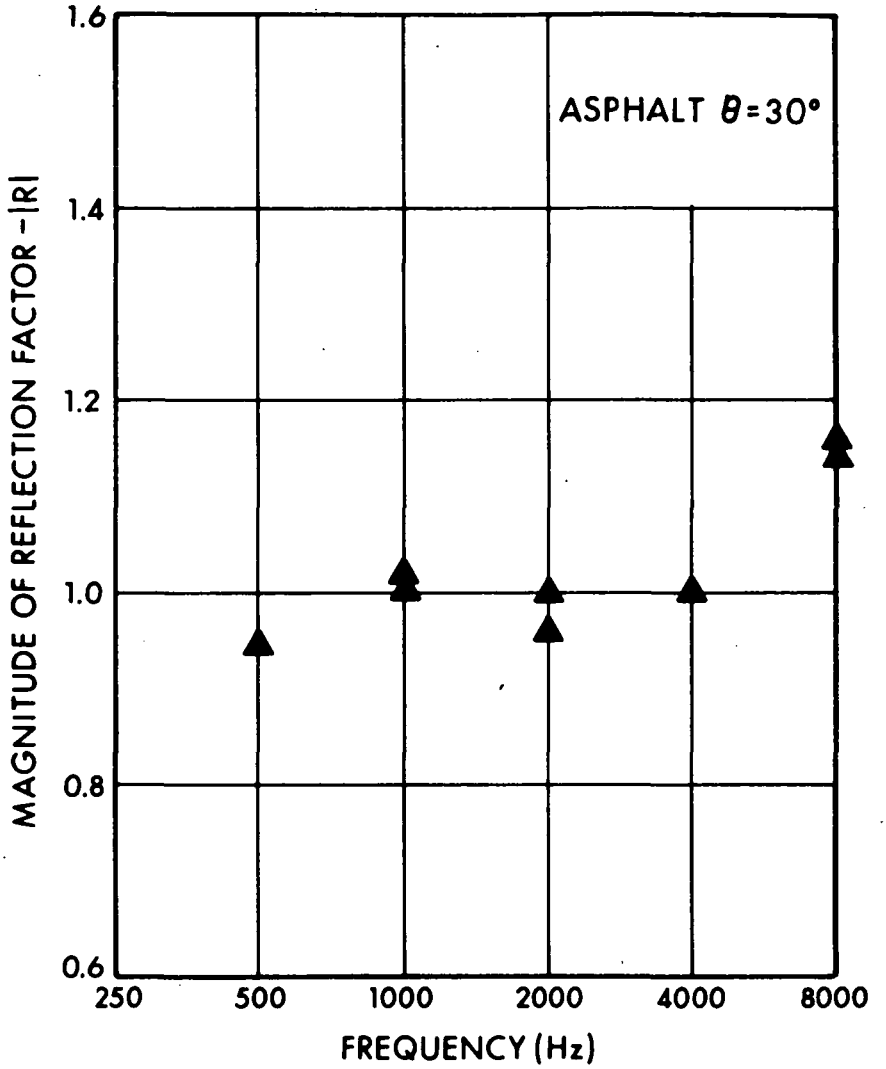

FIG. 17. REFLECTION COEFFICIENT; ASPHALT, θ = 30°.

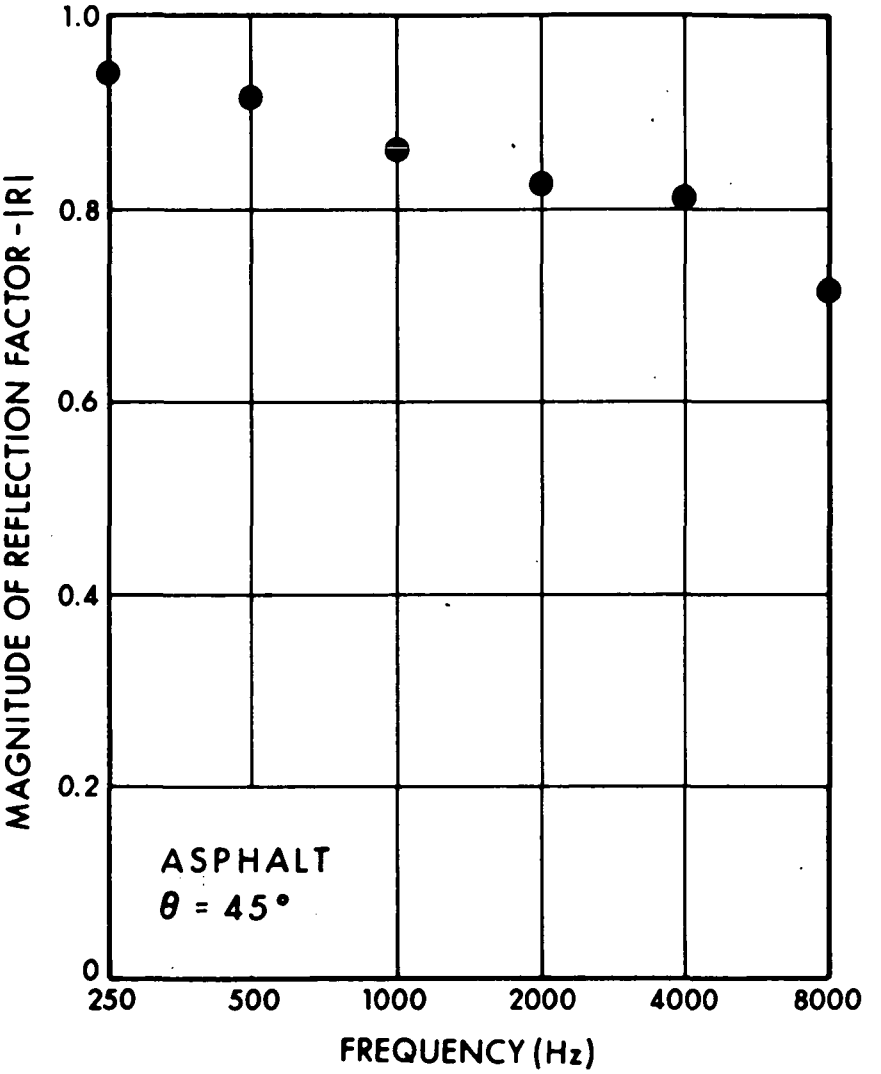

FIG. 18. REFLECTION COEFFICIENT; ASPHALT, θ = 45°.

frequency – a trend not seen in the 30° data. We did not undertake any investigation of this phenomenon, and therefore do not know its cause. Theory (Morse and Ingard, 1968) predicts, however, that the reflection coefficient at a given frequency should increase for incident angles near grazing.

At one frequency band, (the 8000 Hz octave band) (for $\theta = 30°$), the measured reflection coefficient was slightly greater than 1.0. This result would indicate that more acoustic energy is reflected from the asphalt surface than was incident upon it – an impossible result. One explanation for the observed data is that small surface irregularities, with dimensions comparable to shorter wavelengths, created a slight focusing effect that caused a reflected ray of greater amplitude than that reflected from a true plane surface.

SECTION 5

SUMMARY AND CONCLUSIONS

Measurements of the reflection factor were made in an anechoic chamber using two different techniques. The first method used a correlator and a point source emitting a pure tone, and was intended to determine both the amplitude and phase of the reflection factor. The measured values of the phase were erratic and could not be repeated, despite extensive efforts to refine the technique.

The second method used for the indoor measurements was the phase cancellation method – a variation of the technique used previously by Vér and Myles (1973). Data obtained over a limited range of frequencies for two surfaces, concrete and asphalt, showed considerable scatter. This scatter is attributed to the disturbing effects of sound diffracted from the edges of the samples, whose size was limited by the dimensions of the anechoic chamber. The reflection coefficient for concrete was found to be about 1.0, while that of asphalt was lower, about 0.8 between 2000 and 6000 Hz.

Outdoor measurements of the reflection coefficients of asphalt and grass-covered soil were made using the filtered random noise correlation method because of its insentisivity to ambient noise. Here again, a correlator was used, but this time in conjunction with a noise source emitting white noise filtered in bandwidths of one octave. The technique thus measured the reflection coefficient averaged over an octave, rather than at a single frequency. The averaging ability of the correlator made the techniques much less sensitive to ambient noise, allowing its use in outdoor environments.

Between 500 and 4000 Hz, the reflection coefficient of grass drops off considerably with increasing frequency, while that of asphalt does not. The data obtained outdoors for asphalt compares well with that measured in the anechoic chamber, although there is considerable scatter in the latter data.

Only a small variation in the wind velocity and surface temperature was encountered during the course of the measurements made outdoors, and it had no noticeable effect on the results obtained. This is not surprising, however, since only the magnitude and not the phase of the reflection factor was measured. The primary effect of wind and temperature gradients is to change the length of the propagation paths. This change

is usually small in comparison with the length of the propagation paths themselves, but may be comparable to a wavelength. The phase of the wave reflected off the surface is thus affected much more than its amplitude. Hence, measurements of the phase angle and the reflection factor may be expected to be very sensitive to local meteorological conditions, whereas measurements of the magnitude would be less effected by these factors.

LIST OF SYMBOLS

A = Acoustic transfer function of sound source (Eq. 2).

$C(\tau)$ = Cross-correlation function.

C_1 = Amplitude of cross-correlation function between sound source input and receiver microphone output (no reflecting plane present), (Eq. 5a).

C_2 = Amplitude of cross-correlation function between the sound source input signal and the receiver microphone output signal (reflecting plane in place).

C_r = Amplitude of the cross-correlation function between the input signal to the sound source and that portion of the receiver microphone output which is due to the reflected signal (Eq. 5b).

c = Speed of sound.

D = Complex amplitude of diffracted wave (Eq. 16).

d = Path length of diffracted wave (Eq. 16).

E = Complex amplitude of voltage supplied to sound source.

$e(t)$ = Voltage supplied to sound source.

f = Frequency.

$G(\omega)$ = Power spectral density of input to sound source (Eq. 17).

i = $\sqrt{-1}$

P = Complex amplitude of pressure.

$p(t)$ = Sound pressure.

R = Complex reflection factor.

$Re\{\ \}$ = Real part of quantity in brackets { }.

r = Length of reflected path (Fig. 2).

LIST OF SYMBOLS *(Continued)*

s = Distance from sound source to receiver microphone (Fig. 2).

s_1 = Distance from noise source to source microphone.

T_1 = Time delay (Eq. 6c).

T_2 = Time delay (Eq. 8).

T_r = Time delay (Eq. 6d).

t = Time.

Greek Letters

Δ_{RS} = Error in measuring path length difference r-s.

Δf = Frequency increment.

$\Delta\omega$ = Radian frequency bandwidth.

θ = Sound wave incidence angle (Fig. 2).

λ = Wavelength.

ξ = Delay time (Eq. 20).

τ = Delay time.

ϕ_A = Phase angle of complex transfer function A (Eq. 4b).

ϕ_R = Phase angle of complex reflection factor R.

ω = Radian frequency.

ω_u = Upper limit of frequency band (Eq. 19).

ω_ℓ = Lower limit of frequency band (Eq. 19).

ω_c = Radian center frequency of filter band (Eq. 21).

REFERENCES

American Society for the Testing of Materials, (1972), "Standard Method of Test for Sound Absorption of Acoustical Materials in Reverberation Rooms," designation C423-66 (Reapproved 1972), *1975 Annual Book of ASTM Standards*, Philadelphia.

Embleton, T.F.W., *et al.*, (1974). "Outdoor Sound Propagation Over Ground of Finite Impedance," *J. Acoust. Soc. Amer.* 59(2) 267-277.

Morse, P. and Ingard, K.U. (1968). *Theoretical Acoustics*, McGraw-Hill, New York.

Ver, I.L. and Myles, M.M. (1973). "Acoustical Modeling Study of the Proposed NASA Langley Outdoor Anechoic Test Apparatus," BBN Report No. 2614, prepared under contract NAS1-9559.